IEEE Access
Multidisciplinary | Rapid Review | Open Access Journal

Received November 2, 2018, accepted November 29, 2018, date of publication December 5, 2018,
date of current version December 31, 2018.

Digital Object Identifier 10.1109/ACCESS.2018.2885198

Optimized Interval Type-II Fuzzy Controller-Based STATCOM for Voltage Regulation in Power Systems With Photovoltaic Farm

YING-YI HONG, (Senior Member, IEEE), AND MENG-JU LIU
Department of Electrical Engineering, Chung Yuan Christian University, Taoyuan 32023, Taiwan
Corresponding author: Ying-Yi Hong (yyhong@ee.cycu.edu.tw)

This work was supported by the Ministry of Science and Technology, Taiwan, under Grant 106-2221-E-033-044.

ABSTRACT The intermittent characteristics and high penetration of renewables (such as photovoltaic and wind powers) cause voltage and stability problems in power systems. The static synchronous compensator (STATCOM) has recently acquired attention on account of its ability to regulate system voltages and improve system stability. This paper presents a novel interval type-II fuzzy logic system (IT2 FLS)-based controller, which consists of current and voltage regulators, applied to the STATCOM, to mitigate bus voltage variations caused by large disturbances (such as intermittent generation of photovoltaic arrays). The current regulator is used to produce the phase angle at the voltage-source converter in the STATCOM while the voltage regulator outputs the current reference on the quadrature axis for the STATCOM. The parameters of the upper/lower membership functions and control gains are optimized by particle swarm optimization. A realistic 10-bus distribution system is used to demonstrate the effectiveness of the proposed method. Comparative studies reveal that the proposed method outperforms traditional PI and type-I FLS-based methods.

INDEX TERMS Particle swarm optimization, photovoltaic farm, power systems, STATCOM, type II fuzzy set, voltage regulation.

I. INTRODUCTION

Renewable power generation from large photovoltaic (PV) farms and wind-turbine-generators (WTGs) are attracting much attention because they can mitigate greenhouse gas emissions [1], [2]. However, power generation from PV arrays and WTGs is uncertain and intermittent. A high penetration of PV or wind power is highly likely to cause stability and voltage problems in power systems [3]–[5]. Several methods have been used to mitigate these phenomena, such as utilization of energy storage systems [6], [7].

The static synchronous compensator (STATCOM) is a type of Flexible Alternative Current Transmission System (FACTS), which can regulate the real or reactive power flows in power systems [8]. STATCOM is a VAR source/sink and can be utilized in either an electric transmission or an electric distribution system [9], [10]. Incorporating an energy storage system, STATCOM can also regulate the real power flow in a power system [11].

STATCOMs have been used to study the stability problem. Gounder *et al.* [12] used the reactive power margin of a load bus as an index to identify the location of the STATCOM for enhancing the transient voltage stability of a real distribution network. Darabian and Jalilvand [13] presented a multi-objective predictive control strategy to improve the stability of a power system in the presence of wind farms and a STATCOM. Choi *et al.* presented a special protection scheme for use in Korea's electric power system that involves transient stability enhancement using a STATCOM. The required capacity of the STATCOM was determined by applying the equal area criterion to reduce the number of tripping generators [14].

Recently, the STATCOM has been utilized to solve voltage problems in power systems. Petersen *et al.* [15] presented small-signal-based models of wind turbines and STATCOMs using the state-space approach to design a voltage controller. Kanchanaharuthai *et al.* [16] used a STATCOM and battery energy storage system to enhance transient stability and provide voltage regulation by damping assignment. Varma *et al.* [17] proposed voltage control, together with auxiliary damping control, for use in a grid-connected PV solar farm inverter in a STATCOM to increase transient stability and consequently the power transmission limit.

On the other hand, traditional fuzzy logic system (FLS, also called the type-I (T1) fuzzy rule base) has been employed to design controllers. The T1 FLS has been found to be effective when the controlled plant is not complex. In contrast with T1 FLS, an interval type-II (IT2) FLS is more applicable to a complex system. Type-II fuzzy sets incorporate an additional dimension representing uncertainty in degrees of membership [18]. Liang and Mendel [19] proposed a simplified method to evaluate the input and antecedent operations for the IT2 FLS. Other studies have elaborated on the IT2 FLS [20]–[23].

Recently, the IT2 FLS has been used to solve power system problems. Naik and Gupta [24] used the IT2 FLS, incorporated into a pitch angle controller and a STATCOM, to smooth the output power and regulate the terminal voltage of a wind generator. Yassin *et al.* [25] used an IT2 FLS to control the dc-link voltage of converters for a variable speed synchronous machine (SM) to enhance its the capability of low-voltage ride-through. Mitra *et al.* [26] used an IT2 FLS to calculate the fault rate of each distribution line. Type of fault, fault location and calculated fault rate help operators assess voltage sag in a distribution system.

This work proposes a novel IT2 FLS-based STATCOM to mitigate voltage variations that are caused by intermittent photovoltaic power generation. Responses of the power system are insensitive to parameters of the FLS because the parameters of the membership functions and gains are tuned by particle swarm optimization (PSO). Both current and voltage regulators of the STATCOM are explored. The proposed method is implemented by integrating the MATLAB code (PSO) with Simulink (IT2 FLS and dynamic model of components). The merits of this work are as follows.

1) The parameters of both the voltage regulator and the current regulator are tuned; only one of them is tuned or all are fixed in the current literatures.
2) All nonlinear models of components are fully considered, such as power electronics and pulse-width modulation. Traditional methods may only apply linearized state-space models.
3) The parameters of the IT2 FLS-based STATCOM are tuned by PSO with a limited population size in order to minimize the steady-state error of the responses.
4) Responses of the power system are insensitive to change of the upper/lower membership functions of the proposed IT2-FLS.

The rest of this paper is organized as follows. Section II provides the background of the IT2 FLS. Section III presents the method that is based on the PSO-based IT2 FLS for mitigating the voltage variations. Section IV elaborates the simulation results of a realistic 10-bus distribution system with PV generation. Section V draws conclusions.

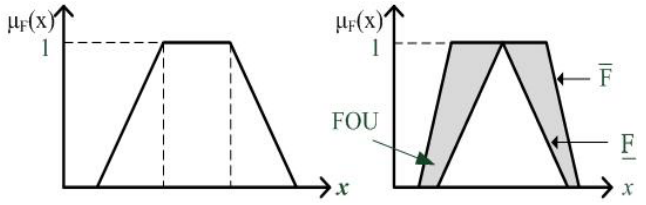

FIGURE 1. (a) T1 membership function and (b) IT2 membership functions.

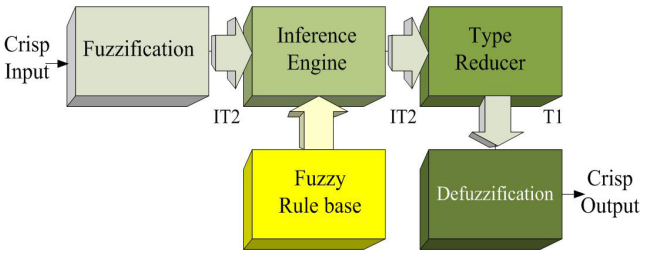

FIGURE 2. IT2 fuzzy logic system [18], [19].

II. T1 AND IT2 FUZZY LOGIC SYSTEMS

A. T1 AND IT2 FUZZY SETS

A conventional fuzzy set, which is also called a type 1 (T1) fuzzy set, $\tilde{F}$ in X, is defined as follows.

$$\tilde{F} = \left\{ \left(x, \mu_{\tilde{F}}(x) \right) | x \in X \right\} \tag{1}$$

where $\mu_{\tilde{F}}(x)$ is the membership function (MF) representing the degree (0∼1) to which x belongs to $\tilde{F}$ and X is the universe of discourse. Figure 1(a) shows a T1 fuzzy set. The MF can be determined either empirically or algorithmically.

The membership values of a conventional T1 fuzzy set are crisp and unambiguous. By contrast, the MFs of an interval type II (IT2) fuzzy set are vague and ambiguous. As illustrated in Fig. 1(b), the value of an IT2 MF is within an interval. Restated, an IT2 fuzzy set is characterized by two T1 MFs, $\bar{F}$ (upper MF, UMF) and $\underline{F}$ (lower MF, LMF). The area between $\bar{F}$ and $\underline{F}$ is referred to as the footprint of uncertainty (FOU). IT2 fuzzy sets are particularly useful when obtaining specific MFs is difficult. IT2 FLS generalizes the standard T1 FLS to enable more uncertainty to be handled in a control system.

B. IT2 FUZZY LOGIC SYSTEMS

Figure 2 displays a block diagram of an IT2 FLS [18], [19]. In the fuzzification block, crisp inputs are applied to the FLS and the degree to which these inputs belong to each of the appropriate fuzzy sets is determined. In the inference engine block, the fuzzified inputs are applied to the antecedents of the fuzzy rules. To evaluate the conjunction (AND) of the rule antecedents, the product operation or intersection is conducted. Two numbers (truth values) are then applied to the consequent UMF and LMF. The outputs of the inference engine remain IT2 fuzzy sets. A type-reducer is used to convert IT2 fuzzy sets into a T1 fuzzy set before defuzzification.

Specifically, let N and M be the numbers of rules and IT2 fuzzy sets, respectively. $\tilde{F}_{in}(i = 1, 2, \ldots, M)$ are IT2 fuzzy sets. The n^{th} rule can be expressed as follows.

IF x_1 is $\tilde{F}_{1n}$ and ... and x_M is $\tilde{F}_{Mn}$, then y is Y_n. $n = 1, 2, \ldots, N$.

where Y_n can be an interval or an IT2 fuzzy set. Let $x^* = (x_1^*, x_2^*, \ldots, x_M^*)$ be the inputs. The IT2 FLS can be realized by the following steps [18], [19].

1) Fuzzification: calculate the degrees of memberships of x^* on each $\tilde{F}_{in}$, $[\mu_{\underline{F}_{in}}(x_i^*), \mu_{\bar{F}_{in}}(x_i^*)]$, $i = 1, 2, \ldots, M$, $n = 1, 2, \ldots, N$.

2) Inference engine: evaluate the firing interval of the n^{th} rule, $F_n(x^*) \equiv [\underline{f}_n, \bar{f}_n]$, $n = 1, 2, \ldots, N$. In this paper, the product operation is utilized to conduct the conjunction of the rule antecedents.

$$[\underline{f}_n, \bar{f}_n] = [\mu_{\underline{F}_{1n}}(x_i^*) \times \ldots \times \mu_{\underline{F}}(x_M^*), \mu\bar{F}_{1n}(x_1^*) \times \ldots \times \mu\bar{F}_{Mn}(x_M^*)] \quad (2)$$

3) Type reducer: Let Y_n be an interval $[\underline{y}_n, \bar{y}_n]$. The elements of sets $\{\underline{y}_n\}$ and $\{\bar{y}_n\}$ are sorted in ascending order. Then type reduction is performed using $F_n(x^*)$ and $[\underline{y}_n, \bar{y}_n]$.

$$y_\ell = \min_{j\epsilon[1,N-1]} \frac{\sum_{n=1}^{j} \bar{f}_n \underline{y}_n + \sum_{n=j+1}^{N} \underline{f}_n \underline{y}_n}{\sum_{n=1}^{j} \bar{f}_n + \sum_{n=j+1}^{N} \underline{f}_n} \quad (3)$$

$$y_r = \min_{j\epsilon[1,N-1]} \frac{\sum_{n=1}^{j} \underline{f}_n \bar{y}_n + \sum_{n=j+1}^{N} \bar{f}_n \bar{y}_n}{\sum_{n=1}^{j} \underline{f}_n + \sum_{n=j+1}^{N} \bar{f}_n} \quad (4)$$

Karnik-Mendel algorithms can be used to estimate y_l and y_r in (3) and (4) [18], [19].

4) Defuzzification: evaluate the defuzzified output.

$$y = \frac{y_\ell + y_r}{2} \quad (5)$$

III. PROPOSED METHOD

A. MODEL OF STATCOM

The main devices in the STATCOM are two capacitors, which provide reactive power. These two capacitors are applied to 4 × 12-pulse three-level inverters, which are connected to four zigzag phase-shifting transformers (−15 deg., −7.5 deg., +7.5 deg., +15 deg.).

The measured three-phase AC voltages and currents (V_{abc} and i_{abc}) are applied to the STATCOM controller. The STATCOM comprises five blocks, which are the Park transform, the voltage regulator, the DC voltage regulator, the current regulator and the phase locked loop (PLL) circuit, as shown in Fig. 3. Specifically, the Park transform performs the abc to dq0 transformation on a set of three-phase signals. It computes the three components (V_d/I_d on the direct axis, V_q/I_q on the quadrature axis, and V_0/I_0 in the zero sequence) in a two-axis rotating reference frame. In the current regulator, as shown in Fig. 4, the error between the current (Iq) on the quadrature axis and its corresponding reference (Iq_{ref}) is applied to a PI controller with gains (kp_1 and ki_1) to produce "alpha" [27], where "alpha" is the phase difference between the AC bus with the voltage-source converter

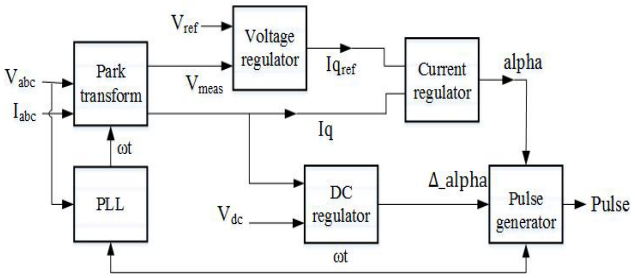

FIGURE 3. STATCOM controller.

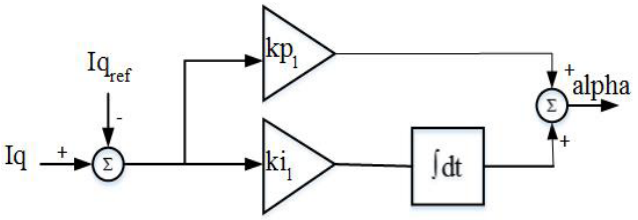

FIGURE 4. Current regulator.

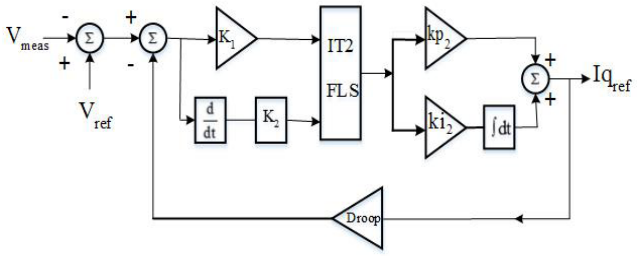

FIGURE 5. Voltage regulator.

and the voltage-regulated bus (denoted as V_{meas} below). In contrast, the voltage regulator, shown in Fig. 5, utilizes the difference between the measured voltage (V_{meas}) and the voltage reference (V_{ref}) as well as a negative feedback signal "Iq_{ref} × Droop" as inputs to produce Iq_{ref}, which affects the reactive power output. Notably, the IT2 FLS is implemented in the voltage regulator. The functions of K1 and K2 act as scaling factors before the IT2 FLS is applied. kp_2 and ki_2 are the PI controller gains in the voltage regulator.

B. IT2 FUZZY RULES FOR CONTROLLERS

This paper proposes an IT2 FLS-based voltage regulator to mitigate the voltage fluctuation, as shown in Fig. 5. The proposed IT2 fuzzy rule is expressed as

IF x_1 is $\tilde{F}_{1n}$ and x_2 is $\tilde{F}_{2n}$ then y is $\tilde{Y}_n$. $n = 1, 2, \ldots, 25$.

where x_1 is $K_1 \times ((V_{ref} - V_{meas}) - Iq_{ref} \times Droop))$ (denoted as "$K_1 \times \Delta e$") and x_2 is the rate of change of $K_2 \times \Delta e$ (that's, $K_2 \times \Delta \dot{e}$). The variable y is the input applied to the PI controller with gains kp_2 and ki_2.

A total of 25 IT2 fuzzy rules are implemented in the proposed method (i.e., N = 25), as shown Table 1. The symbols NL, NS, ZR, PS, and PL, represent "Negative Large", "Negative Small", "Zero", "Positive Small", and "Positive Large", respectively. All UMFs of $\tilde{F}_{1n}$, $\tilde{F}_{2n}$ and $\tilde{Y}_n$

TABLE 1. Twenty-five IT2 fuzzy rules.

	x_1=NL	x_1=NS	x_1=ZR	x_1=PS	x_1=PL
x_2=PL	NL	NL	NL	NS	ZR
x_2=PS	NL	NL	NS	ZR	PS
x_2=ZR	NL	NS	ZR	PS	PL
x_2=NS	NS	ZR	PS	PL	PL
x_2=NL	ZR	PS	PL	PL	PL

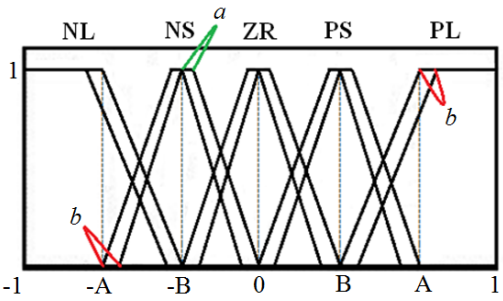

FIGURE 6. Upper and lower membership functions.

are expressed as trapezoid functions, while the corresponding LMFs of NS, ZR and PS are triangular ones, as shown in Fig. 6. The parameters a and b denote the tolerances (uncertainties) between the UMF and the LMF. Restated, the values of a and b influence FOU. Notably, these IT2 membership functions are symmetrical. The right boundaries of fuzziness for $\tilde{F}_{1n}, \tilde{F}_{2n}$ and $\tilde{Y}_n$ are A1, A2 and A3, respectively. The centers of PS for $\tilde{F}_{1n}, \tilde{F}_{2n}$ and $\tilde{Y}_n$ are B1, B2 and B3, respectively. Accordingly, a total of 12 unknown variables must be determined. They are A1∼A3, B1∼B3, kp_1, ki_1, kp_2, ki_2, K_1 and K_2, which are determined by particle swarm optimization (PSO) herein.

C. TUNING PARAMETERS USING PSO

Traditional optimization methods (e.g., gradient decent) cannot be used to tune the parameters A1∼A3, B1∼B3, kp_1, ki_1, kp_2, ki_2, K_1 and K_2 because the objective function is implicit. PSO is adopted herein to determine the above unknowns. PSO is able to explore the global optimum and exploit the local optimums simultaneously. In contrast, other traditional evolutionary algorithms (such as genetic algorithms) are generally regarded as less efficient.

PSO, which is an evolution-based optimization method, utilizes a population of particles (possible solutions), whose historical information is updated iteratively and which move in a ψ-dimensional solution space. Let the superscript t be the iteration index. The position and velocity of each particle p are updated as follows [28].

$$V_p^{t+1} = \omega^t V_p^t + c_1 r_1^t \left(p_{best}^t - X_p^t\right) + c_2 r_2^t (g_{best}^t - X_p^t) \quad (6)$$

$$X_p^{t+1} = X_p^t + V_p^{t+1} \quad (7)$$

where vectors X_p and V_p represent the ψ-dimensional position and velocity of particle p, $p = 1, 2, \ldots, P$ (population size), respectively. The inertia weight ω copies the features of

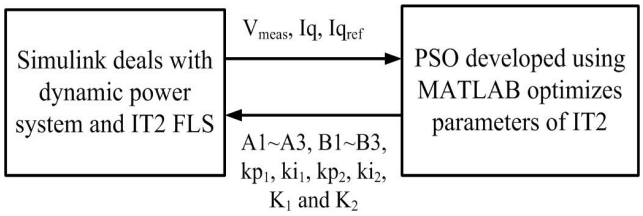

FIGURE 7. Co-simulation conducted by integrating MATLAB with Simulink.

in the preceding iterations to the current iteration. A greater ω corresponds to a stronger impact of preceding V_p^t on V_p^{t+1}.p_{best} and g_{best} mean the best position of a particle at present and the best known position that has been found by any particle in the swarm so far, respectively. The values of r_1 and r_2 are generated randomly within [0, 1]. Learning factors c_1 and c_2 are positive constants within [0, 2] and $c_1 + c_2 \leq 4$. The terms $c_1 \times r_1$ and $c_2 \times r_2$ dominate the velocity of a particle. X_p^{t+1} denotes the p-th vector (particle) at the $(t+1)$-th iteration and V_p^{t+1} can be considered to be the $(t+1)$-th updated value (ΔX_p^{t+1}).

The $c_1 r_1^t \left(p_{best}^t - X_p^t\right)$ term in (6) conducts the local search (exploration) and the $c_2 r_2^t (g_{best}^t - X_p^t)$ term in (6) performs the global search (exploitation) in a ψ-dimensional search space. The global search should coordinate with the local search to avoid premature results and reach the global optimum. The inertia weight ω governs the momentum of the particle and decreases linearly during the iterations, such that PSO initially executes global searches, changing gradually over to local searches.

In this paper, X_p denotes a vector whose elements are A1∼A3, B1∼B3, kp_1, ki_1, kp_2, ki_2, K_1 and K_2. Accordingly, $\psi = 12$. The initial inertia weight ω and population size are 0.92 and 30, respectively. c_1 and c_2 are 1.2 and 0.12, respectively. The fitness (objective) in this study is the total sum of Integral Absolute Errors (IAE) in both the current regulator and the voltage regulator, as follows.

$$\int \left|(V_{ref} - V_{meas}) - I_{qref} * Droop\right| dt + \int \left|I_q - I_{qref}\right| dt \quad (8)$$

D. CO-SIMULATION IN MATLAB AND SIMULINK

MATLAB and Simulink were used to implement the proposed method. The proposed IT2 FLS and the power system were developed in Simulink to simulate dynamic power flow while PSO was coded using MATLAB script, as in Fig. 7.

MATLAB software has interfaces that can be used to link it with Simulink. The dynamic power flow studies are performed in Simulink by solving different systems of differential equations for modeling the components in the power system. V_{meas}, Iq and Iq_{ref}, computed by Simulink, are fed to MATLAB to compute A1∼A3, B1∼B3, kp_1, ki_1, kp_2, ki_2, K_1 and K_2.

The studied problem herein has 12 unknowns, which are the parameters of membership functions and six control gains for a single STATCOM. If more STATCOM controllers are

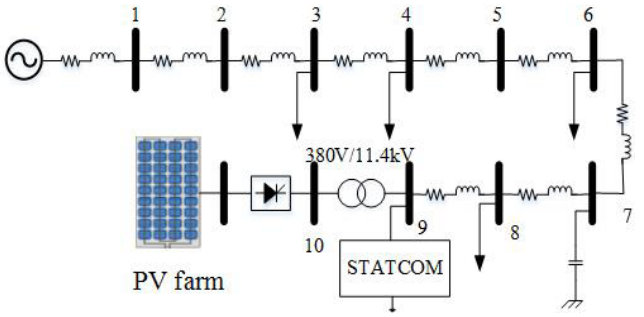

FIGURE 8. Studied system.

studied, the numbers of unknowns and population size in PSO have to be increased. Due to the spaces in substations and consideration of costs in electric power utilities, the number of STATCOM is very limited and identified locations of STATCOMs must have a great impact on system voltages.

The CPU time required for running the co-simulation depends on the number of buses, which are modeled in the Simulink. A distribution STATCOM is generally installed in a feeder of a distribution system, which may consist of many feeders receiving power from individual substations. The structure of a distribution system is radial; a STATCOM installed on a feeder has little impact on the voltages of an adjacent feeder. Accordingly, each feeder can be studied independently. The studied feeder in this paper comprises 10 buses, which is a typical size. For example, the possible maximum number of buses in a feeder of the IEEE 123-bus Test Feeder for system reconfiguration studies is about 15 [29]. Each lateral of a feeder can be aggregated to a single load.

IV. SIMULATION RESULTS

A realistic 10-bus power system in Taiwan, as shown in Fig. 8, is studied in this paper. A PV farm with a generating capacity of 1.8 MW is located at bus 10. An IT2 rule-based STATCOM with a capacity of 5 MVA is located at bus 9. The nominal voltages of the distribution system and the PV farm are 11.4 kV and 380 V, respectively. The capacitor and the total load are 0.6 MVAR and 3.6MW+j1.35MVAR, respectively. The rest of the relevant data are detailed in the appendix. For comparison, the performances that are obtained by the traditional PI and T1 FLS-based STATCOM are also provided.

A. IRRADIATION CHANGING

The irradiation is initially 1000W/m^2, and decreases linearly to 600 W/m^2 from 0.5s to 0.6 s and then increases linearly to 1000 W/m^2 from 1.2 to 1.3 s, as shown in Fig. 9. Figure 10 plots the corresponding real and reactive power generations from the PV farm. Table 2 presents the ranges of the UMF and the LMF for x_1 (that's, $\tilde{F}_{1n}$), x_2 (that's, $\tilde{F}_{2n}$) and $\tilde{Y}_n$. Each membership function is characterized by four numbers, which denote four points in the universe of disclosure. Because the LMFs of NS, ZR and PS are triangular, their

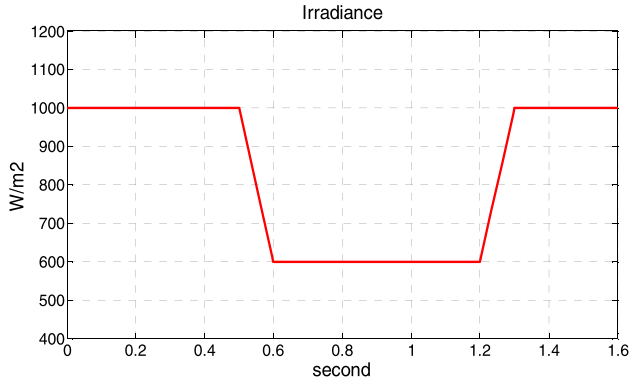

FIGURE 9. Variations of irradiation in studied power system.

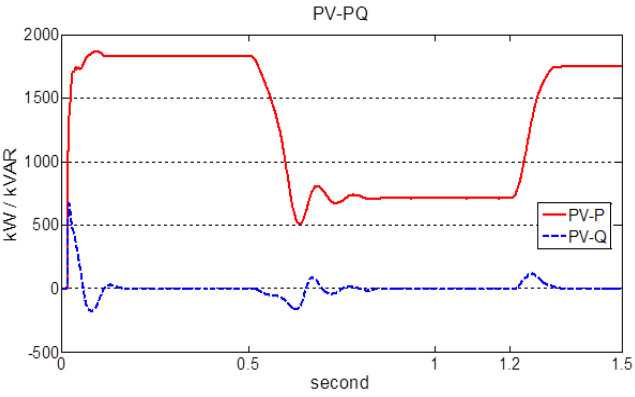

FIGURE 10. Real and reactive power generations.

TABLE 2. Membership functions characterized by four numbers.

		x_1 ($\tilde{F}_{1n}$)	x_2 ($\tilde{F}_{2n}$)	y ($\tilde{Y}_n$)
NL	UMF	[-1,-1,-A1,-B1]	[-1,-1,-A2,-B2]	[-1,-1,-A3,-B3]
	LMF	[-1,-1,-A1-*b*,-B1-*b*]	[-1,-1,-A2-*b*,-B2-*b*]	[-1,-1,-A3-*b*,-B3-*b*]
NS	UMF	[-A1,-B1-*a*,-B1+*a*,0]	[-A2,-B2-*a*,-B2+*a*,0]	[-A3,-B3-*a*,-B3+*a*,0]
	LMF	[-A1+*b*,-B1,-B1,-*b*]	[-A2+*b*,-B2,-B2,-*b*]	[-A3+*b*,-B3,-B3,-*b*]
ZR	UMF	[-B1,-*a*,*a*,B1]	[-B2,-*a*,*a*,B2]	[-B3,-*a*,*a*,B3]
	LMF	[-B1+*b*,0,0,B1-*b*]	[-B2+*b*,0,0,B2-*b*]	[-B3+*b*,0,0,B3-*b*]
PS	UMF	[0,B1-*a*,B1+*a*,A1]	[0,B2-*a*,B2+*a*,A2]	[0,B3-*a*,B3+*a*,A3]
	LMF	[*b*,B1,B1,A1-*b*]	[*b*,B2,B2,A2-*b*]	[*b*,B3,B3,A3-*b*]
PL	UMF	[B1,A1,1,1]	[B2,A2,1,1]	[B3,A3,1,1]
	LMF	[B1+*b*,A1+*b*,1,1]	[B2+*b*,A2+*b*,1,1]	[B3+*b*,A3+*b*,1,1]

2nd and 3rd values are identical. The parameters of a and b, specified in Fig. 6, are 0.01 and 0.05, respectively.

For comparison, the optimal parameters of conventional PI, T1 FLS and the proposed IT2 FLS were attained by individual PSO runs. Figure 11 shows the voltage responses that were obtained by the conventional PI, T1 FLS and the proposed IT2 FLS. Obviously, the voltage gain that was obtained using the proposed method results in the smallest overshoot. As shown in Figure 12, the reactive power output from the STATCOM mitigates the voltage variation caused by intermittent irradiation. The proposed IT2 FLS provides more appropriate reactive power, leading to fast and steady-state responses, than the conventional PI and T1 controllers do. Compared with the benchmark (e.g., conventional PI controller), the proposed method requires off-line

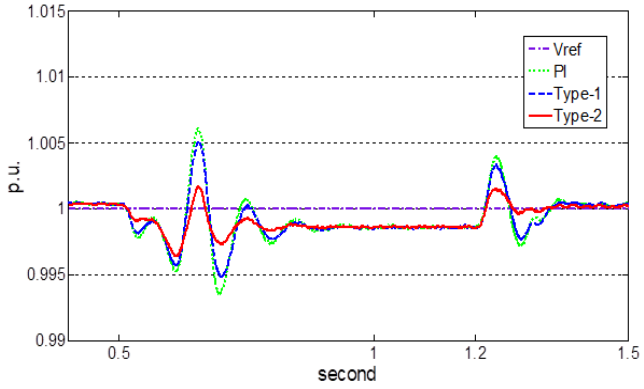

FIGURE 11. Voltage responses obtained by three methods.

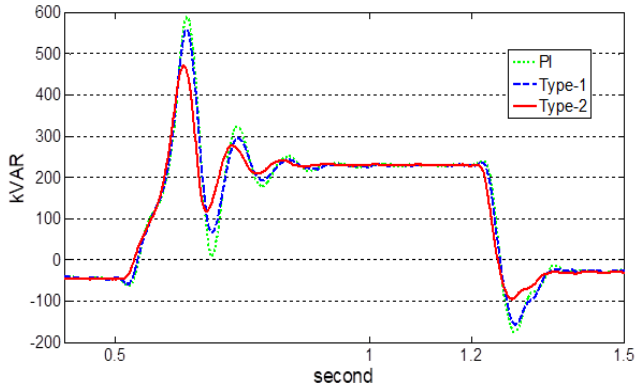

FIGURE 12. Reactive power output from STATCOM.

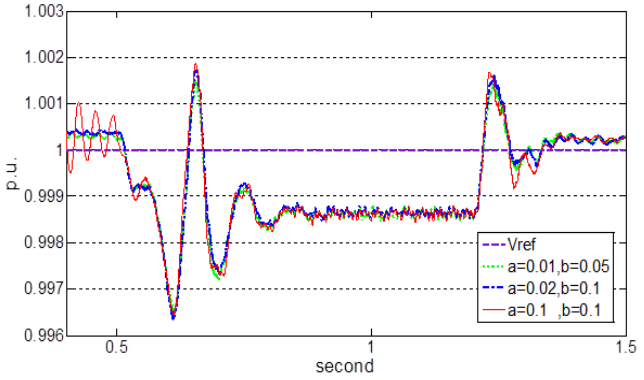

FIGURE 13. Three voltage responses by considering three different values of a and b.

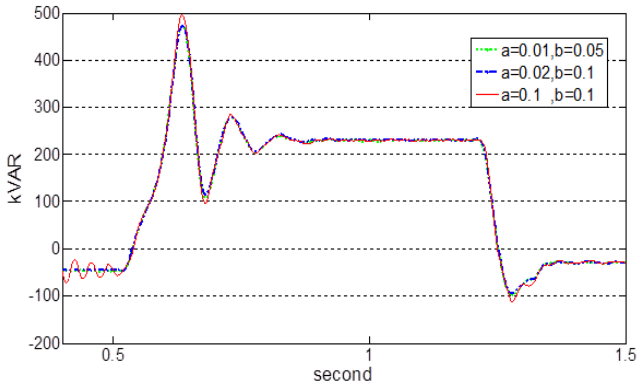

FIGURE 14. Three reactive power responses obtained with three different values of a and b.

parameter tuning and an extra chip to implement IT2 FLS, which is cheap.

B. IMPACT OF PARAMETERS A AND B ON RESPONSES OBTAINED BY PROPOSED IT2-FLS

The study in Sec. IV.A utilizes a = 0.01 and b = 0.05. Figures 13 and 14 display the same scenario as in Sec. IV.A but with (i) a = 0.01, b = 0.05, (ii) a = 0.02, b = 0.1 and (iii) a = 0.1, b = 0.1. The three responses in Figs. 13 and 14 do not appear to differ. These tests confirm that the proposed method is insensitive to different values of a and b, which measure the uncertainty in modeling. Restated, the values of a and b barely affect the FOU. Table 3 shows the optimal solutions obtained by the proposed IT2 FLS, considering various values of a and b. These tests imply that although a and b are set to various values, different optimal A1∼A3, B1∼B3, kp_1, ki_1, kp_2, ki_2, K_1 and K_2 tend to result in similar voltage and reactive power responses.

Small initial oscillations before t = 0.5 s are found in the case with a = b = 0.1, as shown in Figs. 13 and 14. The system stability can be examined by voltage fluctuations (effect), which are caused by the kVAR oscillations (cause). It can be found that the voltage fluctuations are within approximate 0.001 p.u., which actually can be ignored in the operation, and tend to decline gradually. Accordingly, the power

TABLE 3. Optimal solutions considering different values of a and b.

Unknowns	a=0.01, b=0.05	a=0.02, b=0.1	a=0.1, b=0.1
A1	0.9400	0.8996	0.8900
B1	0.5000	0.5000	0.5000
A2	0.9477	0.8900	0.8900
B2	0.5000	0.5000	0.5000
A3	0.9400	0.8900	0.7000
B3	0.5000	0.5000	0.5000
kp_1	1.9218	1.7407	1.2047
ki_1	0.3100	0.2804	0.8388
kp_2	0.3561	0.3816	0.2293
ki_2	0.6328	0.7708	1.1264
K_1	0.5371	0.5453	1.1014
K_2	0.0712	0.4597	1.0354

system is free from instability although the STATCOM produces kVAR oscillations with about peak-to-peak 50 kVAR (about 50/5000 = 1%, which can be ignored, too).

C. IMPACTS OF DIFFERENT OPERATION CONDITIONS ON RESPONSES OBTAINED BY PROPOSED IT2-FLS

The parameters of the upper/lower membership functions and control gains obtained by Sec. IV.A are applied to other operation conditions in this subsection. Because the daily load level is time-varying, system responses of the peak load and off-peak load are examined herein. Total levels of the

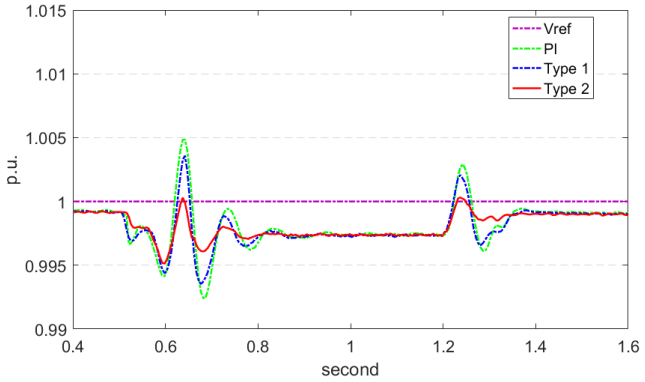

FIGURE 15. Voltage responses obtained by three methods (peak load).

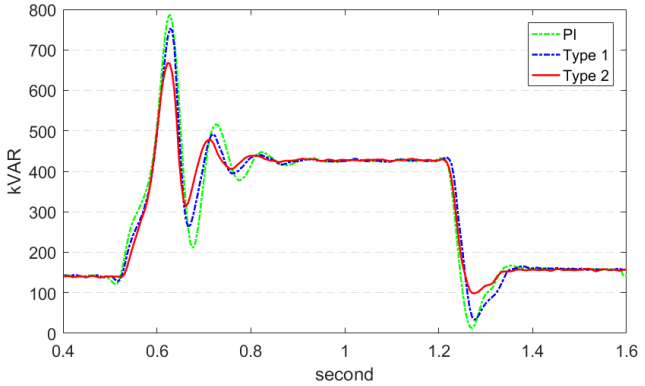

FIGURE 16. Reactive power output from STATCOM (peak load).

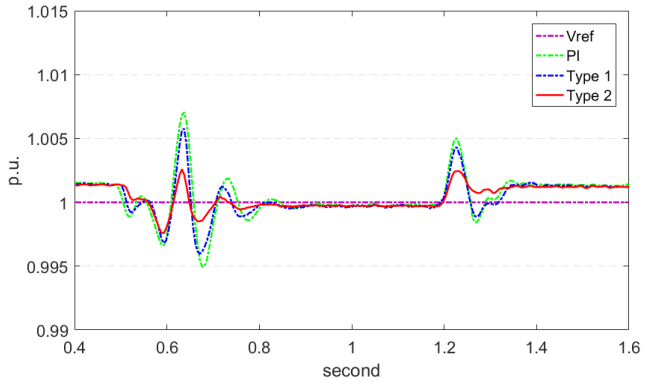

FIGURE 17. Voltage responses obtained by three methods (off-peak load).

peak and off-peak loads are assumed to be 1.5 and 0.5 times (i.e., 5.4MW+j2.025MVAR and 1.8MW+j0.675MVAR) the level of the scenario studied in Sec. IV.A.

Figs. 15 and 16 show the voltage responses and reactive power output of STATCOM for the peak-load case, respectively. Figs. 17 and 18 illustrate the voltage responses and reactive power output of STATCOM for the off-peak-load case, respectively. It can be found that the proposed IT2 FLS-based controller still obtains faster and more stable responses, compared with the conventional PI and T1 FLS-based controllers, in spite of different operation

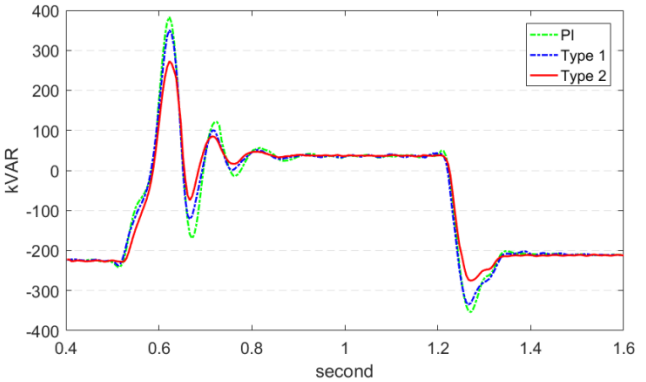

FIGURE 18. Reactive power output from STATCOM (off-peak load).

TABLE 4. Impedance of distribution lines.

Type	Zabc (Ω/km)	Z1 (Ω/km)
3C 500 MCM XP2	$\begin{bmatrix} 0.2536+j0.1464 & 0.1461+j0.0027 & 0.1461+j0.0027 \\ 0.1461+j0.0027 & 0.2536+j0.1464 & 0.1461+j0.0027 \\ 0.1461+j0.0027 & 0.1461+j0.0027 & 0.2536+j0.1464 \end{bmatrix}$	0.1075 + j0.1437
3A 477 XPW (N-1 A300)	$\begin{bmatrix} 0.2103+j0.5908 & 0.0790+j0.2135 & 0.0767+j0.1977 \\ 0.0790+j0.2135 & 0.2152+j0.5649 & 0.0790+j0.2722 \\ 0.0767+j0.1977 & 0.0790+j0.2722 & 0.2103+j0.5908 \end{bmatrix}$	0.1249 + j0.3142

TABLE 5. Lengths and types of distribution lines.

Line		Length (m)	Types
From bus	To bus		
1	2	2100	3C500XP2
2	3	600	3A477XPW
3	4	600	3A477XPW
4	5	900	3C500XP2
5	6	3900	3A477XPW
6	7	2200	3A477XPW
7	8	1000	3A477XPW
8	9	700	3A477XPW

conditions. The reactive power required by the proposed method to stabilize the voltage is the smallest among three methods.

V. CONCLUSIONS

An interval type-II (IT2) fuzzy logic system (FLS)-based STATCOM is proposed in this paper to reduce voltage variations caused by large disturbances (e.g., variation of PV power) in a power system. A realistic 10-bus distribution system is employed to verify the effectiveness of the proposed method. The merits of the proposed method are summarized as follows.

(1) The parameters of UMF/LMF in FLS and the control gains of voltage/current regulators are tuned by particle swarm optimization (PSO). Traditionally, those were specified, only control gains were tuned or only membership functions were tuned.

TABLE 6. Bus loads (Y-grounded connection).

Bus	Real power (MW)	Reactive power (MVAR)
3	1.25	0.50
4	1.25	0.50
6	0.80	0.25
8	0.30	0.10

(2) The simulation results indicate that the optimized IT2 FLS is more applicable to nonlinear and dynamic systems than the traditional T1 FLS and PI controllers because the UMF and LMF are able to deal with uncertainty in systems. Restated, the proposed method outperforms the traditional T1 FLS and PI controllers of the STATCOM.

(3) The nonlinear models and PWM of converter/inverter in the PV farms and STATCOM are fully considered. Traditional methods may only utilize linearized models to reduce computational time, leading to unpredictable numerical errors.

The theoretical contributions of this paper are as follows:

(1) Despite the shapes of the UMF and the LMF, the responses of system are very alike. Changing the FOU has no obvious effect on the response once the control gains and parameters of the membership functions are optimized.

(2) Twenty five IT2 fuzzy rules are proposed. Symmetrical UMF and LMF are also presented to reduce the number of unknowns solved by PSO; thus, the required population size of PSO is small.

APPENDIX

The parameters of the STATCOM that are used in this paper are as follows: secondary side voltage 2.9 kV, resistances of primary zig-zag windings $r_1 = r_2 = 0.0016$ p.u., inductance of primary zig-zag windings $L_1 = L_2 = 0.05$ p.u., $Cp = C_m = 3000\mu$F., and total size 5 MVA.

The parameters of the PV farm are as follows. Under the standard test condition, current at maximum power point $I_m = 4.7$A, short-circuit current $I_{sc} = 4.95$A, voltage at maximum power point $V_m = 35$ V, and open-circuit voltage $V_{oc} = 44$ V. The numbers of modules in parallel and in series are 270 and 48, respectively.

Tables 4 and 5 provide distribution line data for the studied system. Table 6 shows the bus loads.

REFERENCES

[1] B. Currie *et al.*, "Flexibility is Key in New York," *IEEE Power Energy Mag.*, vol. 15, no. 3, pp. 20–29, May/Jun. 2017.

[2] S. Repo *et al.*, "The IDE4L project: Defining, designing, and demonstrating the ideal grid for all," *IEEE Power Energy Mag.*, vol. 15, no. 3, pp. 41–51, May/Jun. 2017.

[3] J. Jung, A. Onen, R. Arghandeh, and R. P. Broadwater, "Coordinated control of automated devices and photovoltaic generators for voltage rise mitigation in power distribution circuits," *Renew. Energy*, vol. 66, pp. 532–540, Jun. 2014.

[4] M. Hasheminamin, V. G. Agelidis, A. Ahmadi, P. Siano, and R. Teodorescu, "Single-point reactive power control method on voltage rise mitigation in residential networks with high PV penetration," *Renew. Energy*, vol. 119, pp. 504–512, Apr. 2018.

[5] J. D. Watson, N. R. Watson, D. Santos-Martin, A. R. Wood, S. Lemon, and A. J. V. Miller, "Impact of solar photovoltaics on the low-voltage distribution network in New Zealand," *IET Gener., Transmiss. Distrib.*, vol. 10, no. 1, pp. 1–9, 2016.

[6] O. Babacan, W. Torre, and J. Kleissl, "Siting and sizing of distributed energy storage to mitigate voltage impact by solar PV in distribution systems," *Sol. Energy*, vol. 146, pp. 199–208, Apr. 2017.

[7] R. Luthander, D. Lingfors, and J. Widén, "Large-scale integration of photovoltaic power in a distribution grid using power curtailment and energy storage," *Solar Energy*, vol. 155, pp. 1319–1325, Oct. 2017.

[8] H. Liao and J. V. Milanović, "On capability of different FACTS devices to mitigate a range of power quality phenomena," *IET Gener. Transmiss. Distrib.*, vol. 11, no. 5, pp. 1202–1211, 2017.

[9] P. N. P. Barbeiro *et al.*, "Sizing and siting static synchronous compensator devices in the Portuguese transmission system for improving system security," *IET Gener., Transmiss. Distrib.*, vol. 9, no. 10, pp. 957–965, 2015.

[10] H. Lee, M. Bae, and B. Lee, "Advanced reactive power reserve management scheme to enhance LVRT capability," *Energies*, vol. 10, no. 10, p. 1540, 2017, doi: 10.3390/en10101540.

[11] M. Beza and M. Bongiorno, "An adaptive power oscillation damping controller by STATCOM with energy storage," *IEEE Trans. Power Syst.*, vol. 30, no. 1, pp. 484–493, Jan. 2015.

[12] Y. K. Gounder, D. Nanjundappan, and V. Boominathan, "Enhancement of transient stability of distribution system with SCIG and DFIG based wind farms using STATCOM," *IET Renew. Power Gener.*, vol. 10, no. 8, pp. 1171–1180, 2016.

[13] M. Darabian and A. Jalilvand, "Improving power system stability in the presence of wind farms using STATCOM and predictive control strategy," *IET Renew. Power Gener.*, vol. 12, no. 1, pp. 98–111, 2018.

[14] D.-H. Choi, S. H. Lee, Y. C. Kang, and J.-W. Park, "Analysis on special protection scheme of Korea electric power system by fully utilizing STATCOM in a generation side," *IEEE Trans. Power Syst.*, vol. 32, no. 3, pp. 1882–1890, May 2017.

[15] L. Petersen, F. Kryezi, and F. Iov, "Design and tuning of wind power plant voltage controller with embedded application of wind turbines and STATCOMs," *IET Renew. Power Gener.*, vol. 11, no. 3, pp. 216–225, 2017.

[16] A. Kanchanaharuthai, V. Chankong, and K. A. Loparo, "Transient stability and voltage regulation in multimachine power systems Vis-à-Vis STATCOM and battery energy storage," *IEEE Trans. Power Syst.*, vol. 30, no. 5, pp. 2404–2416, Sep. 2015.

[17] R. K. Varma, S. A. Rahman, and T. Vanderheide, "New control of PV solar farm as STATCOM (PV-STATCOM) for increasing grid power transmission limits during night and day," *IEEE Trans. Power Del.*, vol. 30, no. 2, pp. 755–763, Apr. 2015.

[18] L. A. Zadeh, "The concept of a linguistic variable and its application to approximate reasoning—I," *Inf. Sci.*, vol. 8, no. 3, pp. 199–249, 1975.

[19] Q. Liang and J. M. Mendel, "Interval type-2 fuzzy logic systems: Theory and design," *IEEE Trans. Fuzzy Syst.*, vol. 8, no. 5, pp. 535–550, Oct. 2000.

[20] C.-F. Juang and C.-Y. Chen, "An interval type-2 neural fuzzy chip with on-chip incremental learning ability for time-varying data sequence prediction and system control," *IEEE Trans. Neural Netw. Learn. Syst.*, vol. 25, no. 1, pp. 216–228, Jan. 2014.

[21] C.-F. Juang and W.-S. Jang, "A type-2 neural fuzzy system learned through type-1 fuzzy rules and its FPGA-based hardware implementation," *Appl. Soft Comput.*, vol. 18, pp. 302–313, May 2014.

[22] Y.-Y. Lin, S.-H. Liao, J.-Y. Chang, and C.-T. Lin, "Simplified interval Type-2 fuzzy neural networks," *IEEE Trans. Neural Netw. Learn. Syst.*, vol. 25, no. 5, pp. 959–969, May 2014.

[23] Y.-Y. Lin, J.-Y. Chang, and C.-T. Lin, "A TSK-type-based self-evolving compensatory interval type-2 fuzzy neural network (TSCIT2FNN) and its applications," *IEEE Trans. Ind. Electron.*, vol. 61, no. 1, pp. 447–459, Jan. 2014.

[24] K. A. Naik and C. P. Gupta, "Output power smoothing and voltage regulation of a fixed speed wind generator in the partial load region using STATCOM and a pitch angle controller," *Energies*, vol. 11, no. 1, p. 58, 2018, doi: 10.3390/en11010058.

[25] H. M. Yassin, H. H. Hanafy, and M. M. Hallouda, "Enhancement low-voltage ride through capability of permanent magnet synchronous generator-based wind turbines using interval type-2 fuzzy control," *IET Renew. Power Gener.*, vol. 10, no. 3, pp. 339–348, 2016.

[26] R. Mitra, A. K. Goswami, and P. K. Tiwari, "Voltage sag assessment using type-2 fuzzy system considering uncertainties in distribution system," *IET Gener., Transmiss. Distrib.*, vol. 11, no. 6, pp. 1409–1419, 2017.

[27] *Optimization Toolbox User's Guide, MATLAB*, MathWorks Inc., Natick, MA, USA, 2017.
[28] J. Kennedy and R. Eberhart, *Swarm Intelligence*. San Mateo, CA, USA: Morgan Kaufmann, 2001.
[29] *Power System Analysis, Computing and Economics Committee*, IEEE 123 Node Test Feeder, IEEE Power Energy Soc., Piscataway, NJ, USA, 1992.

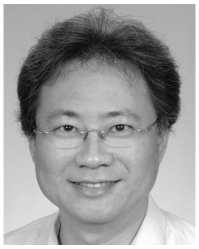

YING-YI HONG received the B.S.E.E. degree from Chung Yuan Christian University (CYCU), Taiwan, in 1984, the M.S.E.E. degree from National Cheng Kung University, Taiwan, in 1986, and the Ph.D. degree from the Department of Electrical Engineering, National Tsing Hua University, Taiwan, in 1990. Sponsored by the Ministry of Education, China, he conducted research at the Department of Electrical Engineering, University of Washington, Seattle, from 1989 to 1990. He has been with CYCU since 1991. His areas of interest are power system analysis and AI applications. He received the Outstanding Professor of Electrical Engineering Award from the Chinese Institute of Electrical Engineering, Taiwan, in 2006. He was the Chair of the IEEE PES Taipei Chapter in 2001.

MENG-JU LIU received the B.S.E.E. degree from Chung Hua University in 2012 and the M.S.E.E. degree from Chung Yuan Christian University in 2016. His research interests include the applications of soft computing and renewable energies.